Microalloying ’25: International Symposium on Microalloying
2–5 June 2025
Vail, Colo., USA
10.33313/302/009

Plate Hot Rolling of Microalloyed Steels: From Metallurgical Mechanisms to Microstructural Modeling

X. Azpeitia[1,2], U. Mayo[1,2], N. Isasti[1,2], P. Uranga[1,2]

[1]CEIT-Basque Research and Technology Alliance (BRTA), Materials and Manufacturing Division

[2]Univ. of Navarra-Tecnun, Mechanical and Materials Engineering Department
20018 Donostia-San Sebastián, Basque Country, Spain
Email: xazpeitia@ceit.es; umayo@ceit.es; nisasti@ceit.es; puranga@ceit.es

INTRODUCTION

The advancement of microalloyed steels over the past five decades has been instrumental in enhancing the mechanical performance and processing efficiency of structural and high-strength steels. Since the MicroAlloying’75 conference, significant progress has been made in understanding the role of microalloying elements [1,2]—particularly niobium (Nb), titanium (Ti), and molybdenum (Mo)—in refining microstructures and improving mechanical properties [3]. The continued evolution of thermomechanical processing (TMCP) strategies, including controlled rolling and accelerated cooling, has enabled the precise tailoring of microstructures to meet the increasing demands of modern steel applications [4].

Plate rolling, a crucial industrial process for producing heavy-gauge steels, presents unique challenges and opportunities in optimizing the interplay between deformation, recrystallization, and precipitation. The controlled introduction of Nb, Ti, and Mo influences grain size, phase transformations, and precipitation behavior, directly impacting the final mechanical properties [5]. Modern computational tools, such as MicroSim, now allow for detailed microstructural predictions, integrating empirical metallurgical models into industrial processing control [6].

MicroSim model was developed in Ceit and has been intensively upgraded for the last years. One of the peculiarities of the model is that the simulation of the microstructural evolution during rolling provides as an output the austenite grain size distributions instead of mean grain sizes. The model has currently different versions for flat (Plate Mill, Hot Strip Mill, Steckel Mill, Thin Slab Direct rolling mills) as well as for long products (Bars and H-Beams Mills). New functionalities and tools were recently included such as the integration of PhasTranSim, the phase transformation model, as well as a thermal model for the estimation of temperature profiles during rolling and cooling. By integrating advanced metallurgical models with industrial rolling schedules, the software provides insights into microstructural homogeneity through-thickness caused by temperature and strain gradients and helps for optimized alloy grade/processing condition definition.

This work bridges fundamental metallurgical understanding with the latest advances and functionalities of modeling tools, enabling the development of high-performance steels while supporting energy-efficient and sustainable production practices.

Keywords: physical metallurgy; Niobium; Titanium; Molybdenum; microstructural modeling

CONSIDERATIONS ON SOME MICROALLOYING ELEMENTS AND SIMULATIONS

To evaluate the microstructural evolution of microalloyed steels during plate rolling, several representative use cases are defined (see Table I). These cases are designed to explore the interactions of alloy composition and processing parameters, providing a basis for validating MicroSim predictions. These use cases will be simulated using MicroSimPM v10.3 to provide insights into the microstructural evolution during processing and to assess the suitability of different alloying strategies for industrial applications.

Nb Microalloying for Structural Applications

Niobium is one of the most versatile elements when referring to microalloying. The most relevant effect during hot working might be the delay, or even complete stop, of static recrystallization kinetics. Two main mechanisms cause this effect: First, Nb is one of the most efficient atoms exerting a solute drag effect to the static recrystallization kinetics; Second, usually at lower rolling temperatures, Nb(C,N) strain induced precipitation might stop static recrystallization, pancaking the austenite grains and providing a powerful ferrite refinement during low temperature transformations due to an increase in specific grain boundary area for nucleation [7,8].

Table I. Summary of the examples for simulations

Use Case	Composition	Rolling Conditions	Objectives/Tools
Nb Microalloying for Structural Applications	0.08%C-1.5%Mn-xNb	High Roughing T: Reheating at 1225°C, Low Roughing T: Reheating at 1150°C	Investigate Nb role in recrystallization control and microstructural pancaking, combining microalloying and processing conditions. - *MicroSim PM, PhasTranSim*
Nb-Ti Microalloying for Pipeline Applications	0.06%C-1.6%Mn-0.08%Nb-0.014%Ti-0.1%Mo	Initial reheating at 1245°C, rough rolling down to 1150°C, rolling temperature 875°C	Analysis of thermal gradients, reduction penetration, through-thickness homogeneity. - *MicroSim PM, Temperature Model, Through-thickness analysis*
Mo (micro)alloying for Direct Quenching of High-Strength plates	0.16%C-1%Mn-xMo-(0.02%Nb)-20ppmB	20mm plate, TMCP, Direct Quenching	Assess the influence of Mo on austenite conditioning by solute drag, bainitic transformation, hardenability. - *MicroSim PM, PhasTranSim*

Possibly with a lower level of relevance, Nb is an effective grain growth control element too, both as a precipitate or in solid solution [9]. This effect could be observed in two different stages of the rolling process. During the reheating furnace, Nb might control austenite grain growth by precipitation pinning effect at relatively low reheating temperatures (with partial Nb particle dissolution). Even if the particles in the slab are fully dissolved due to high reheating temperatures, Nb in solid solution exerts grain growth control decreasing the austenite grain sizes at the exit of the reheating furnace, and therefore, improving the homogeneity of the microstructure during roughing passes. Also, and regarding grain growth during interpass times after static recrystallization, Nb in solution reduces the grain growth kinetics achieving finer microstructures after complete recrystallization between rolling passes when compared to plain CMn steels. This might be especially relevant for plate rolling during the long holding times between roughing and finishing for thermomechanical rolling.

The effective niobium in solution available during rolling will depend on the nominal Nb level added to the steel, the reheating furnace conditions as well as to the presence of other microalloying elements, such as titanium, which could reduce its solubility due to coprecipitation and higher stability of the carbonitrides in the slab [10]. The effective Nb will determine the static recrystallization control by solute drag during roughing passes as well as strain induced precipitation kinetics during fishing passes. The intensity of reductions together with finishing temperatures will determine the amount of Nb in solution at the exit of the rolling. This amount will be a key factor to influence on the transformation kinetics and possible carbide precipitation during cooling stages. Niobium enhances the hardenability promoting the formation of more non-polygonal/acicular ferrite morphologies [11,12]. Depending on the Nb in solution available during transformation some precipitation strengthening could be achieved in the final product [13]. Obviously, achieving an effective precipitation will also depend on C and N contents in solution during finishing.

Based on these general comments, it can be concluded that Nb microalloying is a powerful tool for microstructural control and mechanical property enhancement. Its additions though must be carefully designed, as some of the metallurgical mechanisms acting could result in unexpected cross-mechanism interactions. Therefore, a combined analysis of Nb additions with rolling parameter optimization must be carried out to extract all the benefits from the microalloying element. In this context, MicroSim model could help analyzing the expected outcomes for final microstructures without running costly industrial trials.

Case 1: Effect of Nb During Hot Rolling and Phase Transformations

In the subsequent paragraphs, and based on a real industrial example, the effect of increasing Nb to a base CMn steel will be analyzed for two rolling setups: a high temperature rough rolling and a more optimized low temperature rough rolling design. In addition to MicroSim model to analyze the austenite grain size distribution evolution during rolling, TSoakSim and PhasTranSim modules will also be applied to evaluate the impact on grain size distribution after the reheating furnace and the final microstructure after low temperature phase transformation, respectively.

The schedule used for these simulations reproduces a hot rolling sequence for a 50 mm plate with nine roughing and five finishing passes. The high temperature cycle corresponds to a 1225ºC reheating temperature, while the low temperature one assumes a 1150ºC soaking temperature in the furnace. Considering a base composition of 0.06%C and 1.5%Mn, Table II shows the results of average austenite grain sizes at the exit of the reheating furnace (D_0) after being soaked at different temperatures and a holding time of 60 minutes. The full Nb precipitate dissolution temperature ($Nb_{Sol}T$) is also added for the different chemistries under analysis. From the results, the effect of Nb in solid solution controlling the austenite grain growth during reheating remains clear. The impact of initial coarse grains is more relevant for limited total reductions (slab/plate thickness ratios) as well as microstructure evolution in the centerline area, where reduction penetration is more limited.

Table II. Initial austenite grain size dependence on the chemical composition and soaking temperature predicted by TSoakSim.

	TSoak (°C)	**CMn**	**0.02% Nb**	**0.04% Nb**
$Nb_{Sol}T$ *(°C)*		----	1072	1151
D_0 *(μm)*	1225	183	154	130
	1150	82	72	63

Figure 1 summarizes the results obtained with MicroSim PM model for the high temperature roughing cycle corresponding to the 1225ºC reheating temperature. The Compare tool was used to get a clearer picture of the effect of Nb during rolling. Looking at the recrystallized fraction evolution, the effect of increasing Nb is clear, especially for the 0.04% Nb steel. The lack of recrystallization during almost all the finishing passes is well reflected in the curve (Figure 1a). The CMn and 0.02% Nb steels don't achieve a full pancaking condition during finishing and a mixed microstructure of recrystallized and non-recrystallized grains will be formed during the last passes. This effect has a direct effect on the total accumulated strain or effective pancaking reflected in Figure 1d. Regarding the grain size evolution, the effect of Nb in solid solution as grain growth inhibitor is clearly shown in Figure 1b and c. This effect is well illustrated for the long holding time after the last roughing pass (pass 9). In the case of the CMn steel, the average grain size spikes during the holding time, as the *Dc* value does. *Dc* grain size refers to the cut-off grain size for the 90% accumulated fraction, reflecting somehow the homogeneity of the grain size distribution. For both microalloyed grades, this grain growth during holding at high temperature is hindered, achieving a much finer microstructure entering the finishing stands.

When low temperature roughing cycles are simulated, based on a reheating temperature of 1150ºC, the results plotted in Figure 2 are obtained. In addition to the slight differences observed for the recrystallized fraction and accumulated strain evolutions in Figures 2a and d, the most relevant differences are noted for the average and *Dc* grain size charts in Figures 2b and c, respectively. A significant refinement is clearly observed in all cases, being the contribution of Nb in both refinement and grain size homogeneity especially relevant as Nb levels increase. This effect is well reflected on the *Dc* chart for the 0.04% Nb, controlling the *Dc* values even during the long interpass time between roughing and finishing (pass 9). This trend highlights the effectiveness of Nb in solution as a grain growth controller, offering a valuable approach to maintaining fine and homogeneous microstructures during roughing passes.

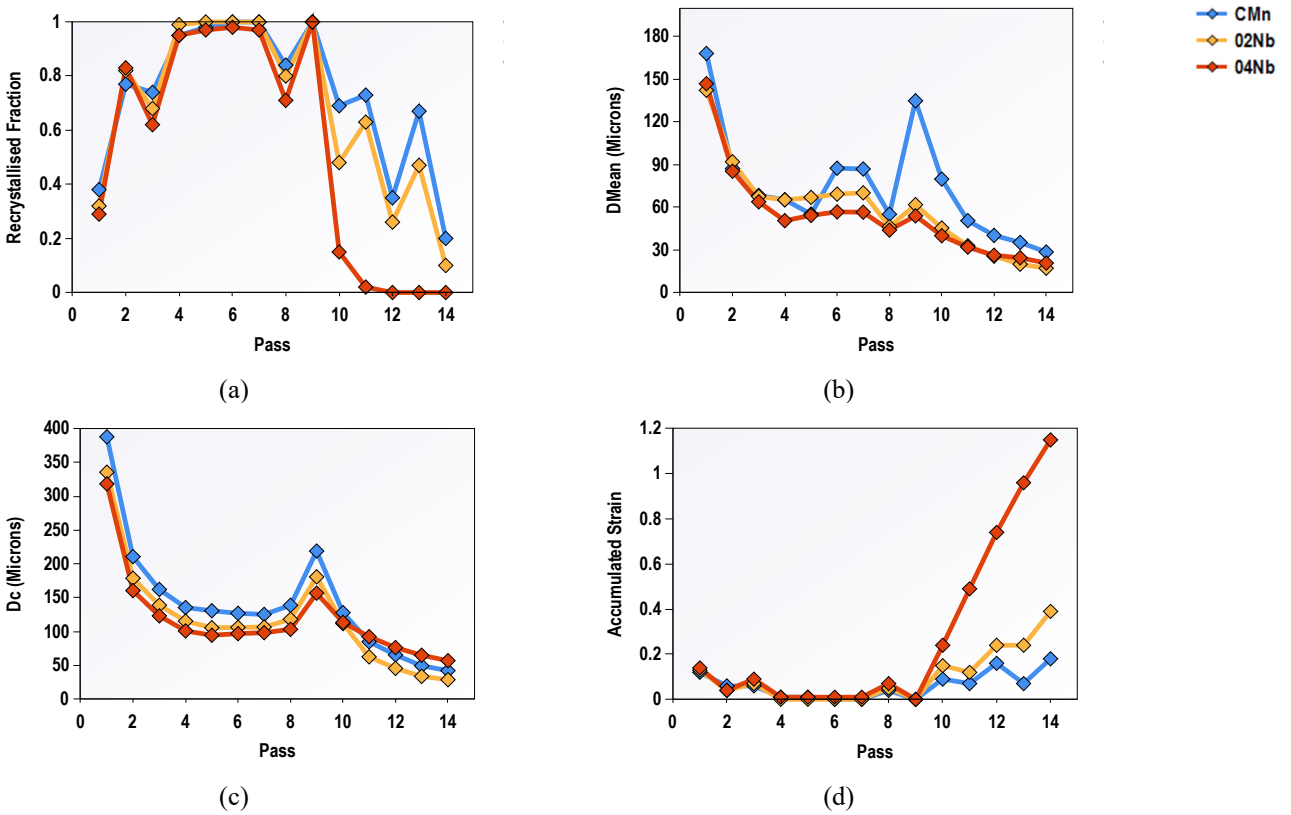

Figure 1: MicroSim Compare results for the high temperature roughing temperature cycle. Evolution of: (a) Recrystallized fraction, (b) Average grain size, (c) *Dc* (90% accumulated cut-off grain size) and (d) Accumulated strain.

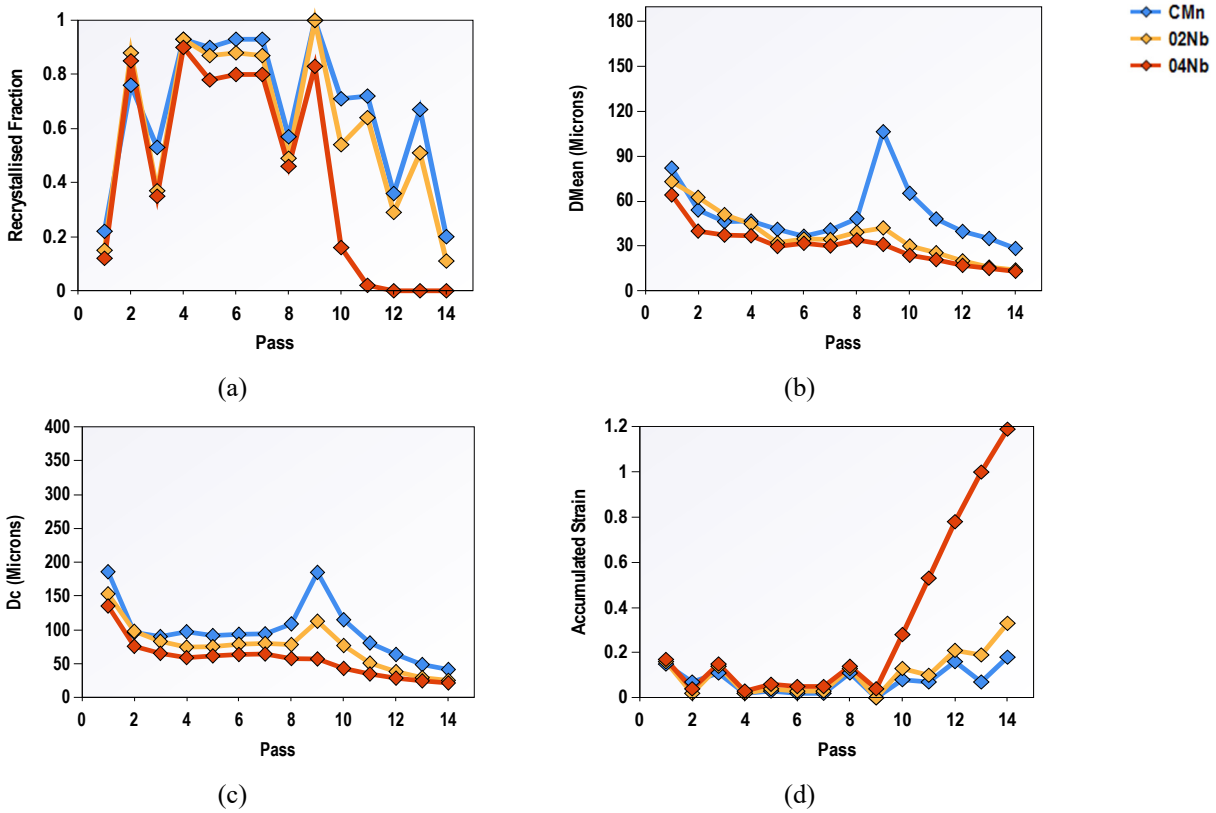

Figure 2: MicroSim Compare results for the low temperature roughing temperature cycle. Evolution of: (a) Recrystallized fraction, (b) Average grain size, (c) *Dc* (90% accumulated cut-off grain size) and (d) Accumulated strain.

An additional output of the model, that could help understanding the effect of Nb during the whole rolling sequence, is the final austenite grain size distribution at the exit of the rolling mill, before phase transformation. The comparison of the three steels for the low rough rolling temperature cycle is shown in Figure 3a. The progressive refinement of the whole grain size distribution as the Nb level increases is evident in the plot. Finally, the model also computes for the Nb in solution evolution during rolling (see Figure 3b). As Nb level increases and the strain induced precipitation activates along the rolling sequence, the amount of Nb in solution decreases progressively. The amount of Nb in solution remaining at the onset of phase transformation will affect the stability of the low temperature phases and will influence the final morphology and size of unit sizes. Nb in solution increases hardenability promoting the formation of more non-polygonal/acicular ferrite grains. Finally, and depending on the amount of Nb and cooling pattern applied, some NbC could be formed providing precipitation strengthening.

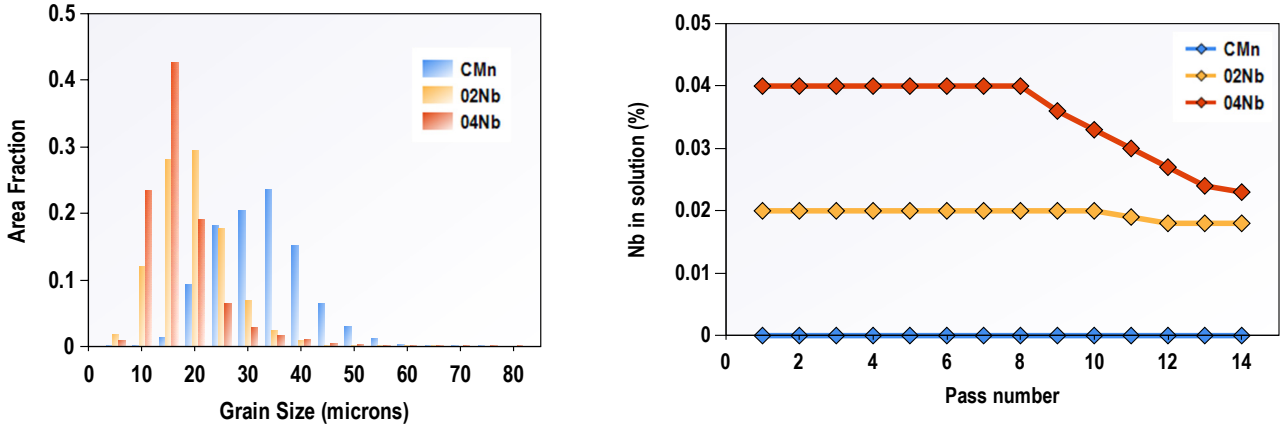

(a) (b)

Figure 3: (a) Final austenite grain size distributions before phase transformation and (b) evolution of the Nb in solution during rolling for the low temperature roughing cycle.

Table III summarizes the predictions by PhasTranSim model considering a constant cooling rate of 1ºC/s at the exit of the last finishing pass. PhasTranSim considers as input the final austenite effective grain size (including size and degree of pancaking) as well as the chemical composition of the steel. For Nb in solution, the model incorporates the calculation of the Nb in solution at the exit of the mill given by MicroSim (see Figure 3b).

As observed in the table, only slight differences are predicted by the phase transformation model. These differences are mainly linked to the relative balance of pearlite and bainite volume fractions. Additionally, for Nb microalloyed grades, microstructural refinement and hardness increase is predicted. If the high and low roughing temperature cycles are compared, a lower fraction of bainite is predicted for the Nb bearing steels under the low temperature roughing condition. The higher refinement and homogenization achieved in austenite after the low temperature rough rolling, is also reflected into the minimum grain size value achieved for the 0.04% Nb, reduced from 10.3 to 8.6 µm from high to low rolling temperatures.

Table III: PhasTranSim prediction values for a constant cooling rate of 1ºC/s.

Cycle	Steel	Ferrite fraction (%)	Pearlite fraction (%)	Bainite fraction (%)	Ferrite Grain Size (µm)	Hardness (HV)
High T Roughing	*CMn*	93.7	1	4.3	13.4	149
	0.02%Nb	93.7	2.8	2.5	9.9	160
	0.04%Nb	93.7	1.9	3.4	10.3	168
Low T Roughing	*CMn*	93.7	1	4.3	13.3	148
	0.02%Nb	93.7	4	1.3	9.1	160
	0.04%Nb	93.7	4.5	0.8	8.6	164

Ti(-Nb) Microalloying

Microalloying with titanium (Ti) presents greater complexity compared to niobium (Nb) or vanadium (V) due to its distinct metallurgical behavior [14]. This complexity arises primarily from Ti low solubility in austenite and its strong affinity for combining with interstitial elements such as oxygen and sulfur, as noted in prior studies [15]. These characteristics influence the precipitation kinetics and phase stability of Ti-bearing compounds, differentiating it from Nb and V microalloying systems. The resulting precipitates, including nitrides and carbides, exhibit unique size distributions and thermal stability, which impact the microstructural evolution during thermomechanical processing.

The effectiveness of Ti microalloying is highly dependent on the titanium-to-nitrogen (Ti/N) ratio, which governs the precipitation behavior and yields two distinct scenarios. When Ti/N < 3.42, hypo-stoichiometric relationship, precipitation predominantly occurs as titanium nitrides (TiN), as illustrated in experimental studies [10]. These nitrides form in two stages: larger particles (>0.5 μm) nucleate in the liquid phase or during the final solidification stages of continuous casting, while a finer population emerges post-solidification, capable of interacting with the austenite microstructure, inferring a delay of static recrystallization under specific circumstances [16]. Due to their high formation temperature and low solubility product, TiN particles remain largely undissolved during reheating and hot rolling, resulting in coarser precipitates compared to Nb or V nitrides. Conversely, in hyper-stoichiometric conditions (Ti/N > 3.42), both TiN and titanium carbides (TiC) form, as documented in precipitation analyses [17]. The TiC particles precipitate primarily during cooling after the final hot rolling pass, though under specific conditions, they may form during rolling and influence austenite grain refinement [18]. TiC precipitation strengthening is one of the most effective precipitation strengthening compounds in microalloyed steels. Titanium stability from heat to heat as well as the definition of robust processing and cooling conditions though are challenging in some mills, reducing the stability in final mechanical properties when the strengthening contributions rely mostly on precipitation.

In steels microalloyed with both Ti and Nb, the interplay between these elements further enhances the metallurgical mechanisms governing grain refinement and strengthening. Fine titanium nitrides, forming at high temperatures, effectively pin austenite grain boundaries during reheating, preventing grain growth. Meanwhile, the effects of Nb during hot working were already discussed in the previous section. The combined effect of TiN and Nb(C,N) precipitates results in a synergistic refinement of the microstructure, as TiN particles stabilize the austenite at elevated temperatures, while finer Nb-bearing precipitates exert recrystallization control during subsequent deformation stages.

A final point to consider is that the presence of titanium nitrides (TiN) can lead to a reduction in the effective Nb available for thermomechanically controlled rolling strengthening due to coprecipitation and overlapping solubility effects. Titanium nitrides, which form at high temperatures owing to Ti strong affinity for nitrogen, can act as nucleation sites for the subsequent precipitation of niobium carbonitrides (Nb(C,N)), resulting in the formation of complex (Ti,Nb)(C,N) particles [10]. This coprecipitation depletes the solute Nb concentration in the austenite matrix, as Nb atoms are incorporated into these mixed precipitates rather than remaining available for independent Nb(C,N) formation during lower-temperature processing stages. Additionally, the similar solubility characteristics of Ti and Nb in austenite exacerbate this effect, as the thermodynamic driving force for Nb precipitation is diminished in the presence of stable TiN, particularly under conditions of limited nitrogen availability. Consequently, the intended recrystallization control and dispersion strengthening provided by Nb may be compromised, necessitating careful adjustment of alloy composition and processing parameters to mitigate these interactions and optimize mechanical properties.

Case 2: API X70 Plate Rolling

In this example the synergetic effect of Nb, Ti and Mo will be analyzed using several MicroSim tools. For this purpose, a sequence for a 28.2mm thick API X70 plate rolling is selected. The alloy design is based on a 0.06% C-1.6% Mn-0.08% Nb-0.015% Ti-0.1% Mo chemistry. The Thermal Model included in MicroSim will be applied to predict through-thickness temperature gradients and average through-thickness temperatures starting from measured surface temperatures available in the mill. For the development of pipe grades, the through-thickness homogenization is a key factor affecting toughness properties, especially drop-weight performance. The availability of tools to predict not just local homogeneity but through-thickness homogeneity can be helpful for a successful alloy grade and processing parameter design.

Some plate mills don't have access to advanced temperature models able to predict temperature evolution during rolling. Nor as average temperature values, neither as detailed through-thickness temperature evolution profiles. Thermal gradient from surface to center affects both strain penetration towards the centerline area as well as local microstructure evolution. In some cases, an average through-thickness temperature can be back calculated based on rolling load measurements and Level 2 systems. In many other cases, though, the only reference for temperature evolution are surface temperature measurements given by pyrometers. In those cases, the Temperature Model integrated in MicroSim is a suitable tool to evaluate average through-thickness temperatures as well as local temperature evolution in surface, quarter, and centerline positions.

An interesting method to validate if the predictions of the thermal model are accurate is the Mean Flow Stress (MFS) Analysis tool. MicroSim provides the option for comparing Mechanical MFS, *MFSMech*, values (based on a Sims-Hill modified method and the measured rolling loads) and the Metallurgical MFS, *MFSMet*, values calculated by a modification of the original Misaka

model. Figure 4 shows the outcomes from the model comparing both sets of data, and the results confirm that the temperature model predictions regarding average temperature evolution are accurate. Real temperature values are hidden in the charts for confidentiality reasons. The impact of temperature on the Metallurgical MFS predictions, as well as its effect on the metallurgical evolution influenced by strain accumulation during finishing, serves as a validation tool for both the Temperature model and the MicroSim predictions.

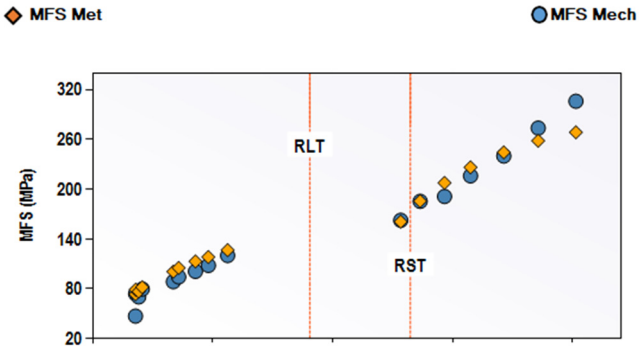

Figure 4. MFS Analysis tool results. Comparison between *MFSMech* and *MFSMet* calculated using the temperature profile predicted by the Temperature model.

Figure 5a shows the temperature profiles calculated by the model. In Figure 5b, the reduction penetration profile calculated by the Through-thickness analysis tools is plotted. From the chart, it can be observed that as the position is closer to the centerline area, the temperature is higher and the degree of effective reduction lower along the whole rolling process. This will influence the local microstructural evolution predictions which will take these values as input parameters.

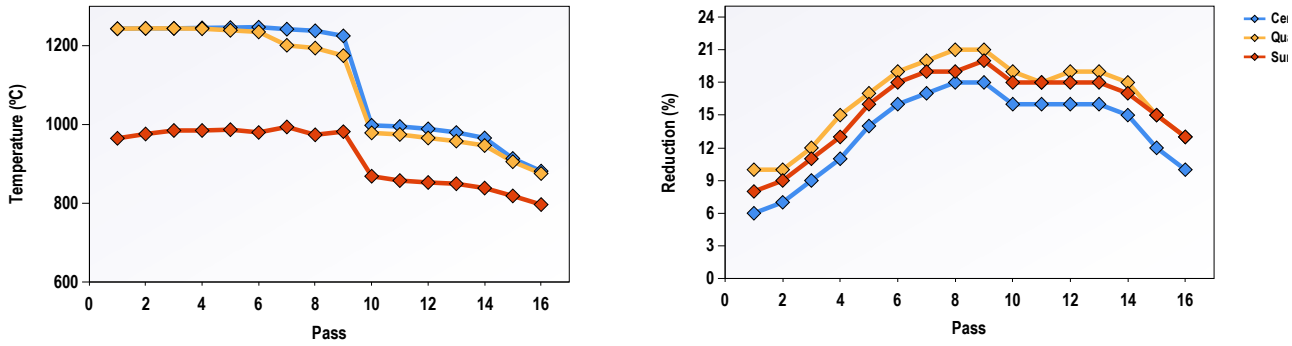

Figure 5. Through-thickness temperature gradients and reduction penetration profiles calculated using the MicroSim Temperature Model as well as the Through-thickness Analysis tool.

Focusing on the specific microstructural evolution differences between quarter and center positions, Figure 6 shows the evolution of various parameters in those positions. From the charts, and in both positions, the recrystallization fraction evolution (Figure 6a) shows a two-stage path, achieving almost complete recrystallization cycles during roughing and a sharp transition to the finishing stands, accumulating a high degree of pancaking. When analyzing grain size evolution, the microstructure at the quarter position is finer (Figure 6b) and more homogeneous (Figure 6c) along the process, compared to that at the center position. Furthermore, some additional strain accumulation is achieved in the quarter position (Figure 6d), providing a more pancaked microstructure. In addition to average sizes, the grain size distributions obtained from the simulation clearly show differences in the width of the distributions, reflecting the presence of coarser grains in the center position when compared to quarter position. This is evident both after the roughing stage (Figure 6e) and at the end of the rolling process, just before transformation (Figure 6f).

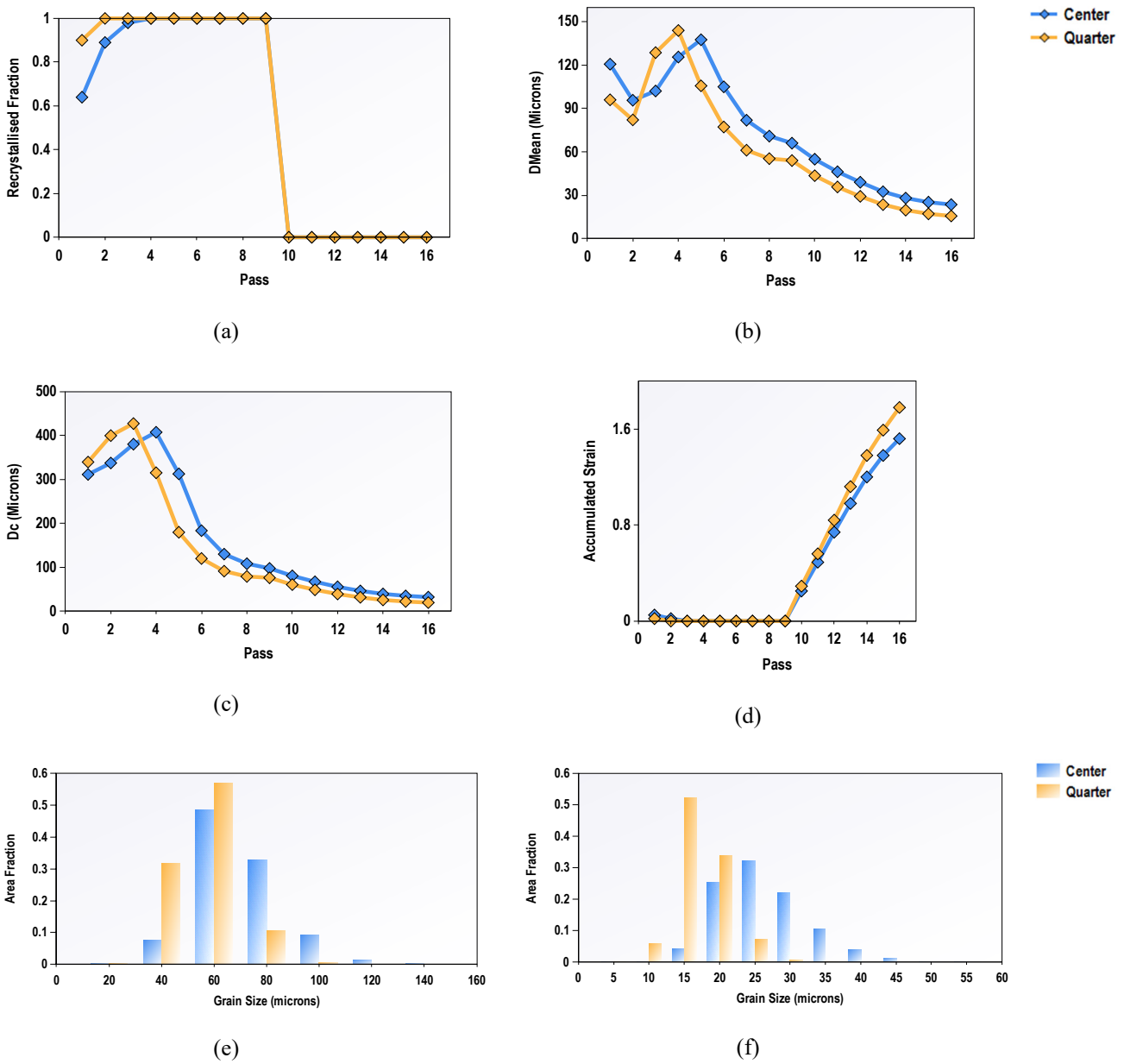

Figure 6. Through-thickness microstructure evolution predictions in quarter and center positions: (a) Recrystallized fraction; (b) Average grain size; (c) *Dc* value; (d) Accumulated strain; (e) Grain size distribution at the entry of the finishing passes; (f) Grain size distribution before phase transformation.

Mo (micro)alloying

Molybdenum microalloying (or alloying if the typical amounts of Mo added are considered) plays a pivotal role in enhancing the mechanical properties of high-strength steels by influencing austenite recrystallization and grain refinement modifying phase transformation [19]. Unlike titanium (Ti) or niobium (Nb), which primarily form stable nitrides or carbonitrides, Mo exerts its effect predominantly through solute drag, retarding the recrystallization of austenite during hot rolling [20]. This retardation arises from Mo segregation to austenite grain boundaries, increasing the activation energy for boundary migration and preserving a finer, pancaked austenite structure prior to cooling. The effect of Mo, delaying static recrystallization kinetics [21] as well as its effect avoiding the onset of dynamic recrystallization [22] has been widely reported in the literature and, for typical alloying additions might be as effective as Nb microalloying. In structural microalloyed grades co-alloyed with Ti and Nb, this effect complements the grain boundary pinning by TiN and Nb(C,N), enhancing the overall refinement of the austenite microstructure, which serves as a foundation for subsequent phase transformations and precipitation strengthening.

During the cooling stage after rolling, Mo significantly influences phase transformation behavior by promoting the formation of bainite and martensite over softer ferrite or pearlite phases. The addition of Mo lowers the bainite start temperature (*Bs*) and increases hardenability by suppressing carbon diffusion, stabilizing austenite and shifting transformation to lower temperatures [23]. This effect is amplified in steels with 0.2–0.5% Mo, where the critical cooling rate for achieving a fully martensitic structure is reduced, enabling less severe quenching while maintaining high strength [24]. In the presence of Ti and Nb, Mo-induced hardenability enhancement ensures a more uniform martensitic matrix, providing an ideal substrate for the precipitation of fine carbides during tempering. This synergy between transformation control by Mo and the microstructural refinement induced by Ti and Nb is critical for optimizing the strength and toughness of quenched and tempered structural steels.

In the tempering stage, Mo contributes to precipitation strengthening through the formation of fine molybdenum carbides (e.g., Mo_2C) and enhances the stability of carbides formed by other microalloying elements. During tempering at 500–600°C, Mo forms nanoscale Mo_2C particles (5–20 nm), which impede dislocation motion and increase yield strength [25]. In structural microalloyed grades containing Nb and Ti, a synergistic effect emerges: Mo stabilizes NbC and TiC precipitates by reducing their coarsening rate, while Nb and Ti, in turn, refine the distribution of Mo_2C by providing additional nucleation sites. This interaction results in a higher density of fine, coherent carbides—such as NbC, TiC, and Mo_2C—compared to single-element systems, boosting precipitation strengthening by 150–250 MPa in optimized compositions. The combined presence of these carbides enhances resistance to softening during tempering, making Ti+Nb+Mo microalloyed steels particularly suitable for high-strength structural applications.

The efficacy of Mo microalloying, and its synergy with Nb and Ti, in quenched and tempered high-strength steels depends on processing parameters and alloy design. In these grades, usually B is added to ensure full quenchability directly after rolling, or during subsequent reaustenitization and quenching steps. Hot-working temperatures of 950–1050°C ensure sufficient Mo solubility in austenite for solute drag, while rapid quenching preserves solute for carbide precipitation during tempering. In Ti+Nb+Mo systems, the sequence of precipitation is critical: TiN forms at high temperatures, pinning grains, followed by NbC and Mo_2C during cooling and tempering, respectively. This sequential precipitation maximizes the volume fraction and stability of carbides, but excessive Mo (>0.5%) or unbalanced Ti/Nb ratios can lead to coarse, incoherent precipitates, reducing toughness. Furthermore, the competitive consumption of carbon by TiC and NbC may limit Mo_2C formation unless carbon content is adequately adjusted. Thus, optimizing alloy composition and thermomechanical processing is essential to harness the full synergistic potential of Nb, Ti, and Mo in enhancing carbide-mediated precipitation strengthening and achieving superior mechanical properties in structural microalloyed grades.

Case 3: B-Mo(-Nb) Microalloyed High Strength Quenched and Tempered Plates

The production of quenched and tempered plates by direct quenching and tempering is a promising route in terms of productivity and final mechanical properties, even if it remains challenging especially when final gauges are thicker. As thickness grows, the effective quenching rate in the quarter/centerline area drops dramatically, increasing the possibility for soft constituent formation and drop in mechanical performance both in strength and toughness. In these situations, the addition of boron is needed [26]. Microalloying with Nb [27] and the addition of other alloying elements such as nickel [28] is also suitable as final properties increase. The understanding of the crossed effects is not straightforward and microstructural evolution modeling to optimize microstructural conditioning before quenching after rolling could be an efficient way to reduce trial costs. In the current example, several simulations were run using MicroSim with increasing alloying contents. Considering a 0.16% C-1% Mn-20ppm B base, two levels of Mo additions were considered, 0.25 and 0.5%, and finally 0.02% Nb was added to the 0.5% Mo bearing steel.

Figure 7 shows the Compare tool results from MicroSim simulations for a 20 mm plate. The mechanisms described in previous sections are clearly illustrated in the charts. On one side, the solute-drag effect of Mo during hot rolling results in lower recrystallized fraction evolution mainly during finishing stands at lower temperatures (Figure 7a). Molybdenum also exerts a grain size control in solid solution reducing grain growth of the recrystallized grains (Figures 7b and c). The combination of solute drag control by Mo and Nb with the onset of Nb(C,N) at low temperatures for the MoNb-bearing steel boosts the strain accumulation to higher levels. The final grain size distributions show a nice trend in austenite refinement and increased homogeneity as alloying levels increase (Figure 7e).

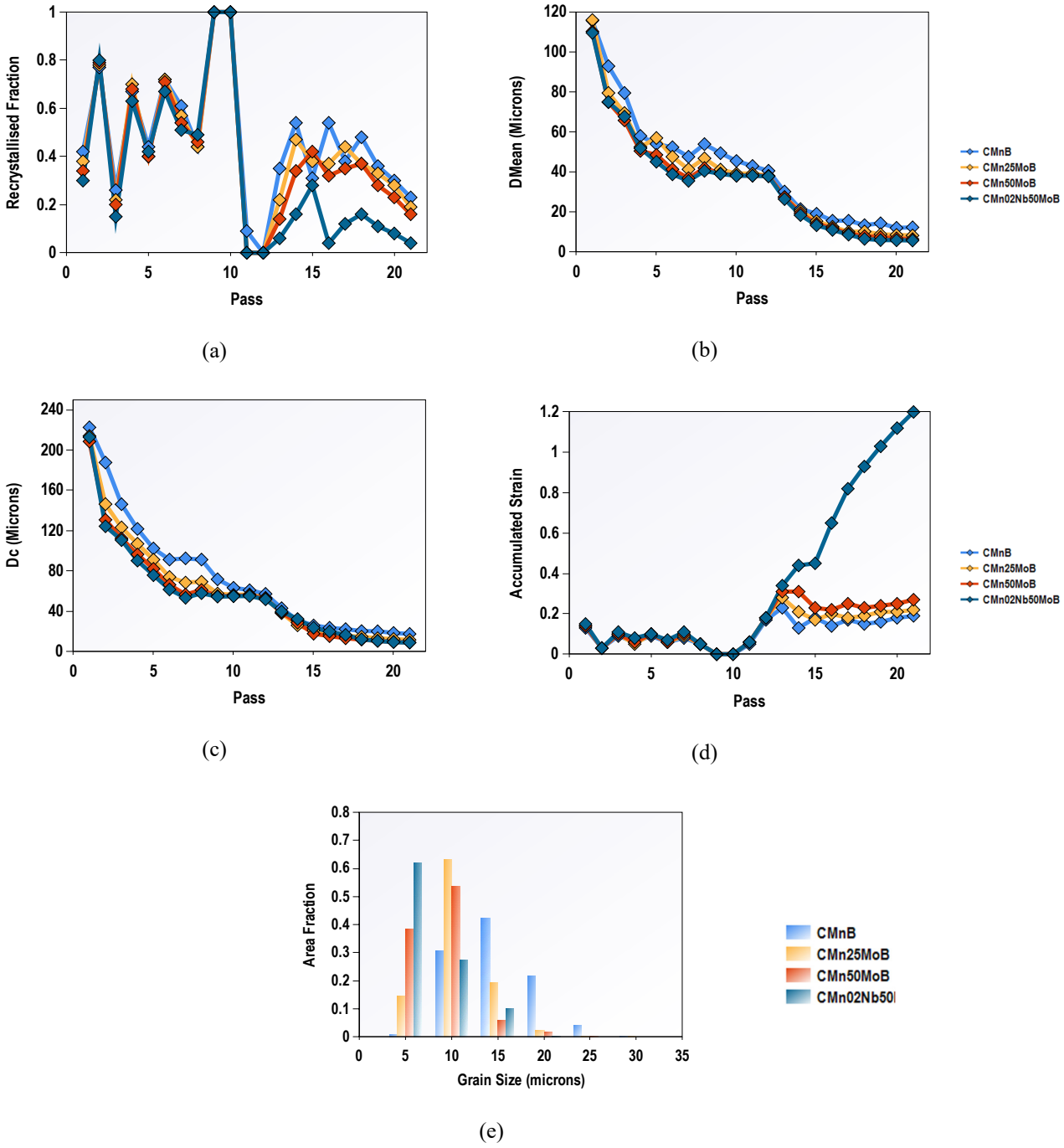

Figure 7. Effect of alloy design on the microstructural evolution predictions. (a) Recrystallized fraction; (b) Average Grain Size; (c) Dc size; (d) Accumulated strain; (e) Austenite grain size distribution before quenching.

PhasTranSim model was used for these grades to predict the effect of alloying elements on the stability of different phases. This way, CCT diagrams were plotted using the model considering the output of MicroSim in terms of alloying content and final austenite microstructure as an input for the simulation. Figure 8 shows the CCT diagrams for the CMnB steel and the alloy with 0.5% Mo added assuming a final austenite grain size of 15 µm. The hardenability increase by the addition of 0.5% Mo is clear, broadening the cooling rate window for full martensitic microstructure formation as well as reducing the probability for ferrite formation. The higher Mo additions also imply an increase in hardness as the martensite/bainite phase balance is modified in the intermediate cooling rate range typical for direct quenching conditions.

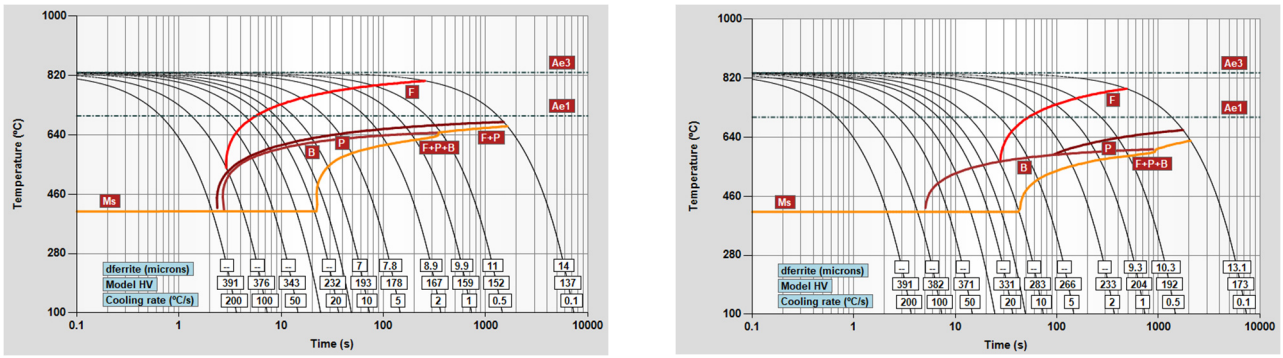

(a) (b)

Figure 8. CCT diagrams predicted by PhasTranSim for: (a) CMnB and (b) CMnB-0.5%Mo steels.

CONCLUSIONS

The study demonstrates the crucial role of microalloying elements—Nb, Ti, and Mo—in controlling microstructural evolution during plate rolling. Niobium enhances recrystallization control, through solute drag and strain-induced precipitation, contributing to grain refinement and improved mechanical properties. The effectiveness of Nb additions is highly dependent on rolling parameters, reheating conditions, and interactions with other microalloying elements, such as Ti. Titanium microalloying, particularly in combination with Nb, improves austenite grain stability at high temperatures and contributes to precipitation strengthening. However, the formation of TiN can reduce the availability of Nb in solution, requiring a controlled steelmaking process, with an adapted alloy design to optimize recrystallization control and final mechanical properties. Molybdenum microalloying significantly influences both hot deformation and transformation behavior. By delaying recrystallization and increasing hardenability, Mo promotes bainite and/or martensite formation in direct-quenched steels. Additionally, Mo enhances precipitation strengthening during tempering by refining carbide distributions, particularly in synergy with Nb and Ti.

The application of the MicroSim modeling platform, including integrated thermal and phase transformation models, enables microstructural predictions throughout the rolling process. Simulations confirm that controlled adjustments to rolling schedules and alloy compositions can enhance through-thickness microstructural homogeneity, optimize transformation kinetics, and reduce reliance on costly industrial trials. Overall, the integration of advanced modeling tools with metallurgical principles supports the development of high-performance, energy-efficient steels, aligning with modern sustainability and industrial competitiveness goals.

ACKNOWLEDGEMENTS

The authors acknowledge the financial support provided by the Basque Government through the Elkartek program (ICME-23 Project, KK-2023/00017). Additionally, they extend their gratitude to CBMM and IMOA for funding research projects that have contributed to most of the results summarized in this manuscript.

REFERENCES

1. J. M. Gray, Preface to MicroAlloying ’75 40th Anniversary Edition, MA-75 Ventures, 2015.
2. M. Cohen and W.S. Owen, Thermo-Mechanical Processing of Microalloyed Steels, Procs. Intl. Symp. High-Strength, Low Alloy Steels, 40th Anniversary Edition, Washington, D.C., 1-3 October, 1975, pp 2.
3. T.N. Baker, Microalloyed steels, Ironmaking Steelmaking, 2016, Vol. 43, pp 264.
4. T. Gladman, D. Dulieu, and I.D. McIvor, Structure-Property Relationships in High-Strength Microalloyed Steels, Procs. Intl. Symp. High-Strength, Low Alloy Steels, 40th Anniversary Edition, Washington, D.C., 1-3 October, 1975, pp 32.
5. G. Larzabal, N. Isasti, J.M. Rodriguez-Ibabe, and P. Uranga, Evaluating strengthening and impact toughness mechanisms for ferritic and bainitic microstructures in Nb, Nb-Mo and Ti-Mo microalloyed steels, Metals, 2017, Vol. 7, 65.

6. C. A. Martins, G. L. de Faria, U. Mayo, N. Isasti, P. Uranga, J. M. Rodríguez-Ibabe, A. L. de Souza, J. A. C. Cohn, M. A. Rebellato and A. A. Gorni, Production of a Non-Stoichiometric Nb-Ti HSLA Steel by Thermomechanical Processing on a Steckel Mill, Metals, 2023, Vol. 13, 405.

7. C. Miao, C. Shang, G. Zhang, and S. Subramanian, Recrystallization and strain accumulation behaviors of high Nb-bearing line pipe steel in plate and strip rolling. Mater. Sci. Eng. A, 2010, Vol. 527, pp 4985.

8. M. Olasolo, P. Uranga, J.M. Rodriguez-Ibabe, and B. López, Effect of austenite microstructure and cooling rate on transformation characteristics in a low carbon Nb–V microalloyed steel, Mater. Sci. Eng. A, 2011, Vol. 528, pp 2559.

9. C. Hutchinson, H. Zurob, C. Sinclair, and Y. Brechet, The comparative effectiveness of Nb solute and NbC precipitates at impeding grain-boundary motion in Nb steels, Scripta Mater., 2008, Vol. 59, pp 635.

10. B. López and J.M. Rodriguez-Ibabe, Some Metallurgical Issues Concerning Austenite Conditioning in Nb-Ti and Nb-Mo Microalloyed Steels Processed by Near-Net-Shape Casting and Direct Rolling Technologies, Met. Mater. Trans. A, 2017, Vol. 48, pp 2801.

11. F. Togashi, and T. Nishizawa, Effect of Alloying Elements on the Mobility of Ferrite/Austenite Interface. J. Jpn. Inst. Met. 1976, Vol. 40, pp 12.

12. N. Isasti, P.M. García-Riesco, D. Jorge-Badiola, M.L. Taheri, B. López, and P. Uranga, Modeling of CCT Diagrams and Ferrite Grain Size Prediction in Low Carbon Nb-Mo Microalloyed Steels, ISIJ Int., 2015, Vol. 55, pp 1963.

13. M.A. Altuna, A. Iza-Mendia, and I. Gutiérrez, Precipitation of Nb in ferrite after austenite conditioning. Part 2: Strengthening contribution in HSLA steels, Met. Mater. Trans. A, 2012, Vol. 43A, pp 4571.

14. J.M. Rodriguez-Ibabe, Optimizing the application of microalloying in value-added steel grades, Online Course, CEIT, 2023.

15. F.B. Pickering, Overview of titanium in microalloyed steels, in Titanium technology in microalloyed steels, Ed. T.N. Baker, London, Institute of Materials, 1997, pp 10.

16. M. Arribas, B. Lopez, and J.M. Rodriguez-Ibabe, Influence of Ti on Static Recrystallization in Near Net Shape Steels, Mater. Sci. Forum, Vol. 500–501, 2005, pp 131.

17. L. García-Sesma, B. López, and B. Pereda, Effect of coiling conditions on the strengthening mechanisms of Nb microalloyed steels with high Ti addition levels, Mater. Sci. Eng. A, 2019, Vol. 748, pp 386.

18. Q. Zhang, L. Li, J. Gao, Z. Li, S. Chen, Z. Peng, and X. Huo, Unraveling the effects of strain–induced precipitation on continuous cooling ferrite transformation in titanium–molybdenum microalloyed steel, J. Mater. Res. Tech., 2024, Vol. 33, pp 906.

19. P. Uranga, C.-J. Shang, T. Senuma, J.-R. Yang, A.-M. Guo and H. Mohrbacher, Molybdenum alloying in high-performance flat-rolled steel grades, Adv. in Manufact., 2020, Vol. 8, pp 15.

20. M.G. Akben, B. Bacroix and J.J. Jonas, Effect of vanadium and molybdenum addition on high temperature recovery, recrystallization and precipitation behavior of niobium-based microalloyed steels, Acta Metall., 1983, Vol. 31(1), pp 161.

21. I. Zurutuza, N. Isasti, E. Detemple, V. Schwinn, H. Mohrbacher and P. Uranga, Effect of Nb and Mo on austenite microstructural evolution during hot deformation in Boron high strength steels, Met. Mater. Trans. A, 2022, Vol. 53A, pp 1529.

22. I. Zurutuza, N. Isasti, E. Detemple, V. Schwinn, H. Mohrbacher and P. Uranga, Effect of Dynamic Recrystallization on Microstructural Evolution in B Steels Microalloyed with Nb and/or Mo, Materials, 2022, Vol. 15, 1424.

23. P. Cizek, B.P. Wynne, C.H.J. Davies, and P.D. Hodgson, The Effect of Simulated Thermomechanical Processing on the Transformation Behavior and Microstructure of a Low-Carbon Mo-Nb Linepipe Steel, Metall. Mater. Trans. 2015, Vol. 46, pp 407.

24. I. Zurutuza, N. Isasti, E. Detemple, V. Schwinn, H. Mohrbacher and P. Uranga, Effect of Quenching Strategy and Nb-Mo Additions on Phase Transformations and Quenchability of High-Strength Boron Steels, JOM, 2021, Vo. 73, pp 3158.

25. I. Zurutuza, N. Isasti, E. Detemple, V. Schwinn, H. Mohrbacher and P. Uranga, Effect of Nb and Mo Additions in the Microstructure/Tensile Property Relationship in High Strength Quenched and Quenched and Tempered Boron Steels, Metals, 2021, Vol. 11, 29.

26. H. Mohrbacher. Property Optimization in As-Quenched Martensitic Steel by Molybdenum and Niobium Alloying. Metals, 2018, Vol. 8, 234.

27. K. Hulka, A. Kern, U. Schriever, Application of Niobium in Quenched and Tempered High-Strength Steels, Mater. Sci. Forum, 2005, Vol. 500–501, pp 519.

28. H. Mohrbacher and A. Kern, Nickel Alloying in Carbon Steel: Fundamentals and Applications, Alloys, 2023, Vol. 2, 1.

